Molecular Pharmacology Fast Forward. Published on December 31, 2008 as doi:10.1124/mol.108.051623
This article has not been copyedited and formatted. The final version may differ from this version.

MOL #51623

Title Page

Anterograde trafficking of G protein-coupled receptors: function of the C-terminal $F(X)_6LL$ motif in export from the endoplasmic reticulum

Matthew T. Duvernay, Chunmin Dong, Xiaoping Zhang, Fuguo Zhou, Charles D. Nichols and Guangyu Wu

Department of Pharmacology and Experimental Therapeutics

Louisiana State University Health Sciences Center, 1901 Perdido St, New Orleans, LA 70112

Molecular Pharmacology Fast Forward. Published on December 31, 2008 as DOI: 10.1124/mol.108.051623
This article has not been copyedited and formatted. The final version may differ from this version.

Running Title Page

Running title: ER export of G protein-coupled receptors

Address correspondence to: Dr. Guangyu Wu, Department of Pharmacology and Experimental Therapeutics, Louisiana State University Health Sciences Center, 1901 Perdido St, New Orleans, LA 70122. E-mail: gwu@lsuhsc.edu

Abbreviations used are: GPCR, G protein-coupled receptor; CT, carboxyl terminus; AT1R, angiotensin II type 1 receptor; AR, adrenergic receptor; ER, endoplasmic reticulum; Ang II, angiotensin II; DMSO, dimethyl sulfoxide; GFP, green fluorescent protein; ERK, extracellular signal-regulated kinase.

Number of text pages: 39

Number of figures: 7

Number of references: 40

Number of words:

Abstract: 247

Introduction: 601

Discussion: 1500

Molecular Pharmacology Fast Forward. Published on December 31, 2008 as DOI: 10.1124/mol.108.051623
This article has not been copyedited and formatted. The final version may differ from this version.

Abstract

We have previously reported that the $F(X)_6LL$ motif in the C-termini essential for export of α_{2B}-adrenergic (α_{2B}-AR) and angiotensin II type 1 receptors (AT1R) from the endoplasmic reticulum (ER). Here we further demonstrated that mutation of the $F(X)_6LL$ motif similarly abolished the cell-surface expression of α_{2B}-AR, AT1R, α_{1B}-AR and β_2-AR, suggesting that the $F(X)_6LL$ motif plays a general role in ER export of G protein-coupled receptors (GPCRs). Mutation of F to V, L, W and Y, and mutation of LL to FF and VV markedly inhibited α_{2B}-AR transport, indicating the $F(X)_6LL$ function cannot be fully substituted by other hydrophobic residues. The structural analysis revealed that the F residue in the $F(X)_6LL$ motif is buried in the transmembrane domains (TM) and possibly interacts with I58 in β_2-AR and V42 in α_{2B}-AR, whereas the LL motif is exposed to the cytosolic space. Indeed, mutation of I58 in β_2-AR and V42 in α_{2B}-AR markedly disrupted cell surface transport of the receptors. Importantly, the V and I residues are highly conserved amongst the GPCRs carrying the $F(X)_6LL$ motif. Furthermore, the F mutant exhibited a stronger interaction with ER chaperones and was more potently rescued by physical and chemical treatments than the LL mutant. These data suggest that the F residue is likely involved in folding of α_{2B}-AR and β_2-AR, possibly through interaction with other hydrophobic residues in neighboring domains. These data also provide the first evidence implying crucial roles of the C-termini possibly through modulating multiple events in anterograde trafficking of GPCRs.

Molecular Pharmacology Fast Forward. Published on December 31, 2008 as DOI: 10.1124/mol.108.051623
This article has not been copyedited and formatted. The final version may differ from this version.

Introduction

G protein-coupled receptors (GPCRs) constitute a superfamily of cell-surface receptors that regulate the cellular responses to a broad spectrum of ligands (Pierce et al., 2002). These GPCRs share common structure features characterized by a core of seven transmembrane-spanning α-helices, three intracellular loops, three extracellular loops, an extracellular N-terminus and an intracellular C-terminus (CT). Whereas the transmembrane core, N-terminus and extracellular loops are involved in ligand recognition, the CT and intracellular loops are involved in the regulation of G protein coupling, phosphorylation and intracellular trafficking (von Zastrow, 2003).

Export from the endoplasmic reticulum (ER) of GPCRs represents the first step in intracellular trafficking of the receptors and influences the cell-surface expression and function of the receptors (Dong et al., 2007; Petaja-Repo et al., 2000). GPCRs are synthesized in the ER. Once correctly assembled and properly folded into their native conformations, the receptors become available for recruitment into ER-derived COPII transport vesicles, which exclusively mediate protein transport from the ER (Dong et al., 2008). It has been well demonstrated that physical interaction of plasma membrane proteins including GPCRs with the ER resident chaperones, such as calnexin and calreticulin, assist the folding and maturation processes to achieve an export competent conformation, and also prevents export of premature cargo proteins (Mizrachi and Segaloff, 2004; Morello et al., 2001). Recent studies have also shown that export of some proteins from the ER is a selective process and is dictated by specific ER export motifs within the cargo proteins. These ER export motifs mediate the interaction of the cargo proteins with components of the COPII transport machinery to facilitate their recruitment into the COPII vesicles, thereby improving the efficiency of ER export (Nishimura and Balch, 1997; Wang et

Molecular Pharmacology Fast Forward. Published on December 31, 2008 as DOI: 10.1124/mol.108.051623
This article has not been copyedited and formatted. The final version may differ from this version.

al., 2004; Ma et al., 2001). The ER derived vesicles are subsequently targeted to the appropriate downstream compartment. As the initial step in post-translational protein biogenesis, the efficiency of ER export influences the kinetics of receptor maturation. Indeed, ER export has been shown to be the rate-limiting step for the maturation of the G protein-coupled δ-opioid receptor (Petaja-Repo et al., 2000).

It has been well appreciated that the membrane-proximal C-terminal region plays an important role in GPCR export trafficking to the cell surface. The requirement of the C-termini for ER export has been demonstrated for a number of GPCRs including rhodopsin, vasopressin V2 (V2R), dopamine D1, adenosine A1, α_{2B}-adrenergic (α_{2B}-AR), angiotensin II type 1 (AT1R), and lutenizing hormone/choriogonadotropin receptors (Duvernay et al., 2004; Heymann et al., 1997; Pankevych et al., 2003). Mutagenesis studies have identified a number of motifs consisting of hydrophobic residues within the membrane proximal C-terminal region which are required for export from the ER (Bermak et al., 2001; Duvernay et al., 2004; Robert et al., 2005; Schulein et al., 1998). However, the molecular mechanism underlying their function in regulating receptor export remains elusive.

We have previously demonstrated that the $F(x)_6LL$ motif in the membrane-proximal C-termini of AT1R and α_{2B}-AR are required for their export from the ER (Duvernay et al., 2004). To define the molecular mechanism underlying the function of the $F(x)_6LL$ motif in mediating GPCR export, we have determined if these residues are involved in receptor dimerization. We have demonstrated that the mutated α_{2B}-AR, in which the F and LL residues in the $F(x)_6LL$ motif were mutated to alanines, forms homo-dimers and hetero-dimers with wide-type α_{2B}-AR and

Molecular Pharmacology Fast Forward. Published on December 31, 2008 as DOI: 10.1124/mol.108.051623
This article has not been copyedited and formatted. The final version may differ from this version.

functions as a dominant negative mutant blocking ER export of its wild-type counterpart (Zhou et al., 2006). In this manuscript we have further characterized the $F(x)_6LL$ motif in GPCRs and elucidated possible molecular mechanisms underlying the function of the $F(x)_6LL$ motif in mediating GPCR export from the ER.

Molecular Pharmacology Fast Forward. Published on December 31, 2008 as DOI: 10.1124/mol.108.051623
This article has not been copyedited and formatted. The final version may differ from this version.

Materials and Methods

Materials. Rat α_{2B}-AR in vector pcDNA3, human β_2-AR in vector pBC, rat AT1R in vector pCDM8 and human α_{1B}-AR tagged with green fluorescent protein (GFP) at its C-terminus were kindly provided by Drs. Stephen M. Lanier, Dr. John D. Hildebrandt (Medical University of South Carolina, Charleston, SC), Kenneth E. Bernstein and Kenneth P. Minneman (Emory University, Atlanta, GA), respectively. Antibodies against GFP, phospho-ERK1/2, calnexin and calreticulin were purchased from Santa Cruz Biotechnology, Inc. (Santa Cruz, CA). Anti-ERK antibodies detecting total ERK1/2 expression were from Cell Signaling Technology, Inc. (Beverly, MA). The α_2-AR agonist UK14304, rauwolscine, dimethyl sulfoxide (DMSO) and protein G-Sepharose 4B were obtained from Sigma-Aldrich (St. Louis, MO). [^{3}H]-RX821002 (specific activity = 41 Ci/mmol), [^{3}H]-CGP12177 (51 Ci/mmol), [7-methoxy-^{3}H]-prazosin (70 Ci/mmol) and [^{125}I]-[Sar1, Ile8]-angiotensin II ([^{125}I]-Ang II) (2200 Ci/mmol) were purchased from PerkinElmer (Waltham, MA). [^{3}H]1-NBMeO (N-[2-methoxy-^{3}H]-(2-methoxybenzyl)-[2-methoxy-^{3}H]-(2,5-dimethoxy-4-iodophenethylamine), a new radioligand with high affinity for serotonin 2 (5-HT$_2$) receptors (Braden et al. 2006) was generously provided by the NIMH Chemical Synthesis and Drug Supply Program. The ER marker pDsRed2-ER was from BD Biosciences (Palo Alto, LA). All other materials were obtained as described elsewhere (Dong and Wu, 2006; Duvernay et al., 2004; Wu et al., 2003).

Plasmid construction. α_{2B}-AR, β_2-AR and AT1R tagged with GFP at their C-termini were generated as described previously (Wu et al., 2003). A similar strategy was used to tag GFP at the C-terminus of 5-HT$_{2C}$ receptor. Our previous studies have shown that the GFP tagging does not influence ligand binding, signaling and trafficking of the receptors (Dong and Wu,

Molecular Pharmacology Fast Forward. Published on December 31, 2008 as DOI: 10.1124/mol.108.051623
This article has not been copyedited and formatted. The final version may differ from this version.

2006, 2007; Dong et al., 2008; Duvernay et al., 2004). Receptor mutants were generated by using the QuikChange site-directed mutagenesis (Stratagene, La Jolla, CA). The sequence of each construct used in this study was verified by restriction mapping and nucleotide sequence analysis (Louisiana State University Health Sciences Center DNA Sequence Core).

Cell culture and transient transfection. HEK293T cells were cultured in Dulbecco's modified Eagle's medium (DMEM) with 10% fetal bovine serum, 100 units/ml penicillin, and 100 units/ml streptomycin. Transient transfection of HEK293T cells was carried out at a cell density of 85-90%, using Lipofectamine 2000 reagent as described previously (Wu et al., 2003). Transfection efficiency for both 6-well and 100-mm dish formats was estimated to be greater than 80% based on the GFP fluorescence.

Intact cell ligand binding. Cell-surface expression of α_{2B}-AR, β_2-AR, AT1R and α_{1B}-AR in HEK293T cells was measured by ligand binding of intact live cells using [^{3}H]-RX821002, [^{3}H]-CGP12177, [^{125}I]-Ang II and [7-methoxy-^{3}H]-prazosin, respectively, as described (Dong and Wu, 2006; Filipeanu et al., 2004, 2006). HEK293T cells cultured on 6-well dishes were transiently transfected with 1.0 μg of plasmids. After 6 h the cells were split into 12-well dishes pre-coated with poly-L-lysine at a density of 5×10^5 cells/well. Twenty-four h post-transfection the cells were serum-starved. Forty-eight h post-transfection, the cells were incubated with DMEM plus [^{3}H]-RX821002, [^{3}H]-CGP12177 or [^{7}Methoxyn-^{3}H]-prazosin at a concentration of 20 nM in a total of 400 μl for 90 min at room temperature to measure the cell surface expression of α_{2B}-AR, β_2-AR and α_{1B}-AR, respectively. The binding was terminated and excess radioligand eliminated by washing the cells twice with ice-cold DMEM. All of the retained radioligand was

Molecular Pharmacology Fast Forward. Published on December 31, 2008 as DOI: 10.1124/mol.108.051623
This article has not been copyedited and formatted. The final version may differ from this version.

then extracted by digesting the cells in 1M NaOH for 2 h at room temperature. The liquid phase was collected and suspended in 5 ml of Ecoscint A scintillation fluid (National Diagnostics Inc., Atlanta, GA). The amount of radioactivity retained was measured by liquid scintillation spectrometry.

For measurement of AT1R expression at the cell surface, HEK293T cells were incubated with 400 µl DMEM containing ^{125}I-Ang II at a concentration of 20 pM for 2 h. After washing the cells twice with 1 ml DMEM, the bound ligand was extracted by mild acid treatment (2 × 5 min with 0.5 ml buffer containing 50 mM glycine, and 125 mM NaCl, pH 3). The radioactivity was counted in a γ-counter. The non-specific binding of α_{2B}-AR, β_2-AR, α_{1B}-AR and AT1R was determined in the presence of rauwolscine (10 µM), alprenolol (20 µM) and phentolamine (10 µM) and nonradioactive Ang II (10 µM), respectively. All radioligand binding assays were performed in triplicate.

Ligand binding of membrane preparations: HEK293T cells were grown on 15-cm diameter tissue culture plates and transfected with 20 µg of plasmid for wild type and mutated receptors for 48 h. Membrane preparations and ligand binding of α_{2B}-AR were performed as described previously (Duvernay et al., 2004). For radioligand binding of $5HT_{2C}$ receptor, total membrane protein was incubated with [^{3}H]1-NBMeO at a saturating concentration of 1 nM in a 600 µl reaction volume of binding buffer containing 50 mM Tris, 10 mM $MgCl_2$, pH7.4. Nonspecific binding was determined in the presence 100 µM mianserin (Tocris, Ellisville, MO).

Fluorescence microscopy. For fluorescence microscopic analysis of receptor subcellular localization, HEK293T cells were grown on coverslips pre-coated with poly-L-lysine in 6-well

Molecular Pharmacology Fast Forward. Published on December 31, 2008 as DOI: 10.1124/mol.108.051623
This article has not been copyedited and formatted. The final version may differ from this version.

plates and transfected with 500 ng of GFP-tagged receptors. For co-localization of GFP-tagged receptors with the ER marker DsRed2-ER, HEK293T cells grown on coverslips were transfected with 500 ng of GFP-tagged receptors and 300 ng of pDsRed2-ER. The cells were fixed with 4% paraformaldehyde-4% sucrose mixture in PBS for 15 min and stained with 4, 6-diamidino-2-phenylindole for 5 min. The coverslips were mounted, and fluorescence was detected with a Leica DMRA2 epifluorescent microscope as described previously (Dong and Wu, 2006; Wu et al., 2003). Images were deconvolved using SlideBook software and the nearest neighbor deconvolution algorithm (Intelligent Imaging Innovations, Denver, CO).

Structural analysis of the F(X)$_6$LL motif in β_2-AR and α_{2B}-AR. A model of the α_{2B}-AR was constructed using the newly published high resolution crystal structure of human β_2AR (pdb code 2rh1) (Cherezov et al., 2007; Rosenbaum et al., 2007). The sequence of α_{2B}-AR was threaded onto the β_2-AR/T4-lysozyme chimera structure based on a sequence alignment generated in Clustal W. The alignment of the 7 TMs in addition to the 8th helix of the cytosolic C-terminal domain were assured manually using DeepView/Swiss PDB viewer. The Swiss-model workspace was then used to submit the file to the Swiss-model automated structure homology-modeling server under "project optimize mode" for energy minimization (Arnold et al., 2006). The resulting file was then loaded into pymol to generate detailed renderings of the model. The pdb file 2rh1 was directly loaded into pymol to generate detailed images of the structure of the human β_2-AR.

Co-immunoprecipitation of α_{2B}-AR and ER chaperones. HEK293T cells cultured on 100-mm dishes were transfected with GFP-tagged α_{2B}-AR or its mutants for 48 h. The cells were

Molecular Pharmacology Fast Forward. Published on December 31, 2008 as DOI: 10.1124/mol.108.051623
This article has not been copyedited and formatted. The final version may differ from this version.

washed twice with phosphate-buffered saline (PBS), harvested and lysed with 500 μl of lysis buffer containing 50 mM Tris-HCl, pH 7.4, 150 mM NaCl, 1% NP-40, 0.5% sodium deoxycholate, 0.1% SDS and Complete Mini protease inhibitor cocktail. After gentle rotation for 1 h at 4^{o}C, the samples were centrifuged for 15 min at 14,000 × g and the supernatant was incubated with 50 μl of protein G-Sepharose for 1 h at 4°C to remove non-specific bound proteins. The samples were then incubated with 5 μg of anti-GFP antibodies overnight at 4 °C with gentle rotation followed by an incubation with 50 μl of protein G-Sepharose beads for 5 h as described previously (Dong and Wu, 2006). After the resin was collected and washed 2 times with lysis buffer without SDS, 100 μl of 2 × SDS-PAGE loading buffer was added to the beads and boiled in a Spin-prep Column (Sigma-Aldrich) for 10 min. Thirty μl from each sample was then separated by SDS-PAGE to probe for calnexin and calreticulin in the GFP-immunoprecipitates by immunoblotting. In parallel, each sample was further diluted 5 times with 1 × SDS-PAGE loading buffer, separated by SDS-PAGE and probed with GFP antibody to determine the amount of the receptor in the immunoprecipitates.

Chemical and low temperature rescue. HEK293T cells are cultured in 6-well dishes and transfected with GFP-tagged α_{2B}-AR for 24 h as described above. The cells were incubated with DMSO at a concentration of 2% in a total of 2 ml of DMEM without fetal bovine serum for an additional 24 h. For low temperature rescue, the cells were cultured at 30^{o}C for 40 h as described previously (Dong and Wu, 2006). The cell-surface expression of α_{2B}-AR was then measured by ligand binding in intact live HEK293 cells using [^{3}H]-RX821002 as described above.

Molecular Pharmacology Fast Forward. Published on December 31, 2008 as DOI: 10.1124/mol.108.051623
This article has not been copyedited and formatted. The final version may differ from this version.

Measurement of cAMP production. cAMP concentrations were measured by using cAMP enzymeimmunoassay system (Biotrak, Amersham Pharmacia Biotech, Piscataway, NJ) as described previously (Dong and Wu, 2007; Filipeanu et al., 2006). HEK293T cells were cultured in 100-mm dishes and transfected with 3 μg of β_2-AR or its mutants tagged with GFP. After 6 h, the cells were split into 12-well plates and cultured for 12 h. The cells were then starved for 24 h and then incubated with isobutylmethylxanthine (0.1 mM) for 30 min before stimulation with ISO at a concentration of 10 μM for 5 min at room temperature. The reactions were stopped by aspirating the medium and the cells were lysed using 200 μl of dodecyltrimethylammonium (2.5%). One hundred μl of cell lysate was transferred into microtitre plates and incubated with anti-cAMP antiserum, followed by the incubation with cAMP-peroxidase conjugate. After washing and addition of substrate, peroxidase activity was measured by spectrometry.

Measurement of ERK1/2 activation. HEK293T cells cultured on 6-well dishes were transfected for 36-48 h. The cells were then starved for at least 3 h before stimulation with the agonist UK14304 at a concentration of 1 μM for 5 min as previously described (Wu et al., 2003). The stimulation was terminated by addition of 300 μl 1 x SDS gel loading buffer. After solubilization of the cells, 20 μl of sample was separated by 12% SDS-PAGE. Activation of ERK1/2 was determined by measuring the level of ERK1/2 phosphorylation with a phosphospecific ERK1/2 antibody. Blots were then stripped and reprobed with total ERK1/2 specific antibodies to confirm equal loading.

Immunoblotting. Western blot analysis of protein expression was carried out as previously described (Dong and Wu, 2007; Wu et al., 2003). HEK293T cell lysates were

Molecular Pharmacology Fast Forward. Published on December 31, 2008 as DOI: 10.1124/mol.108.051623
This article has not been copyedited and formatted. The final version may differ from this version.

separated by SDS-PAGE and transferred onto polyvinylidene difluoride membranes. The signal was detected using ECL Plus (PerkinElmer Life Sciences) and a Fuji Film luminescent image analyzer (LAS-1000 Plus) and quantitated using the Image Gauge program (Version 3.4).

Statistical Analysis. Differences were evaluated using Student's *t* test, and $P < 0.05$ was considered as statistically significant. Data are expressed as the mean ± S.E.

Molecular Pharmacology Fast Forward. Published on December 31, 2008 as DOI: 10.1124/mol.108.051623
This article has not been copyedited and formatted. The final version may differ from this version.

Results

The $F(X)_6LL$ motif is required for the ER export and cell surface transport of α_{2B}-AR, AT1R, α_{1B}-AR and β_2-AR. We have previously demonstrated that mutation of the F and LL residues spaced by six residues [$F(X)_6LL$] in the membrane proximal CT (Fig. 1A) markedly block the cell-surface expression of α_{2B}-AR and AT1R as measured by ligand binding of membrane preparations and subcellular distribution of the receptors (Duvernay et al., 2004). To further confirm the function of the $F(X)_6LL$ motif in mediating their transport to the cell surface, α_{2B}-AR and AT1R and their mutants (α_{2B}-ARm and AT1Rm) in which the F and LL residues in the $F(X)_6LL$ motif were mutated to alanines were transiently expressed in HEK293T cells and the cell-surface expression of the receptors were measured by ligand binding in intact live cells, which will accurately measure the number of receptors at the plasma membrane and eliminate possible contamination with intracellular organelles of membrane preparations. The cell-surface expression of α_{2B}-ARm and AT1Rm were dramatically reduced by 88 and 91%, respectively, as compared with their wild types (Fig. 1B). In contrast, mutation of the $F(X)_6LL$ motif did not significantly alter the overall receptor expression (Fig. 1B). These data are consistent with our previous data demonstrating an essential role of the $F(X)_6LL$ motif in α_{2B}-AR and AT1R transport to the cell surface.

As the $F(X)_6LL$ motif is highly conserved in many family A GPCRs (Fig. 1A) (Duvernay et al., 2004), we then asked if the $F(X)_6LL$ motif is also important for ER export of α_{1B}-AR and β_2-AR. Similar to the effect on the transport of α_{2B}-AR and AT1R, mutation of the F356 and IL362/363 residues in α_{1B}-AR (α_{1B}-ARm) and mutation of F332 and LL339/340 in β_2-AR (β_2-ARm) inhibited their cell surface expression by 87% and 85%, respectively, without altering

Molecular Pharmacology Fast Forward. Published on December 31, 2008 as DOI: 10.1124/mol.108.051623
This article has not been copyedited and formatted. The final version may differ from this version.

total receptor expression as compared with wild-type receptors (Fig. 1B). Consistent with the dramatic attenuation of cell surface expression, cAMP production in response to stimulation of ISO was markedly inhibited in cells expressing β_2-ARm compared with cells expressing wild-type β_2-AR (Fig. 1C).

Analysis of the subcellular localization of the receptors by fluorescence microscopy showed that α_{1B}-ARm and β_2-ARm were unable to reach the cell surface and were extensively accumulated in the periunclear region (Fig. 1D). To further evaluate if the $F(X)_6LL$ motif modulates α_{1B}-AR transport at the level of the ER, α_{1B}-AR and its mutant were expressed together with the ER marker DsRed2-ER and their co-localization was then analyzed. As anticipated, α_{1B}-AR did not significantly co-localize with DsRed2-ER and was expressed at the cell surface, which was confirmed by co-localization with tetramethylrhodamine-conjugated concanavalin A, a plasma membrane marker (data not shown). In contrast, α_{1B}-ARm was strongly co-localized with the ER marker DsRed2-ER (Fig. 1E). Similar results were obtained in cells transfected with β_2-ARm (data not shown). These data suggest that the $F(X)_6LL$ motif may function as a common signal dictating ER export of multiple GPCRs.

Effect of substitution of the F and LL residues in the $F(X)_6LL$ motif with other hydrophobic residues on α_{2B}-AR transport to the cell surface. To determine the physiochemical requirements for the F and LL residues to perform their functions in mediating GPCR export from the ER, we mutated the F and LL residues in the $F(X)_6LL$ motif of α_{2B}-AR to different hydrophobic residues. Each mutation's ability to substitute for the F and LL residues was determined by measuring cell surface receptor expression by intact cell ligand binding and

Molecular Pharmacology Fast Forward. Published on December 31, 2008 as DOI: 10.1124/mol.108.051623
This article has not been copyedited and formatted. The final version may differ from this version.

subcellular distribution. Mutation of the F436 residue to V, L, W and Y significantly impaired α_{2B}-AR transport to the cell surface (Fig. 2A). F436 is substituted best by Y with ligand binding at 32% of α_{2B}-AR. F436V, F436L and F436W mutants bound ligand less than 15% that of α_{2B}-AR (Fig. 2A). Consistent with ligand binding, subcellular distribution analysis showed that F436Y partially expressed at the cell surface, whereas the majority of the F436V, F436L and F436W mutants were retained inside the cell (Fig. 2B). Similarly, mutation of the IL443/444 residues to dihydrophobic VV and FF residues also markedly impeded α_{2B}-AR export to the cell surface as revealed by intact cell ligand biding (Fig. 2A) and subcellular localization (Fig. 2B). These results indicate that the role of the F436 and IL443/444 residues can not be fully substituted by other hydrophobic residues and suggest that F436 and IL443/444 have unique properties which are required for proper modulation of export from the ER of newly synthesized α_{2B}-AR.

Structural analysis of the F(X)$_6$LL motif in β_2-AR and α_{2B}-AR. To provide insights into the molecular mechanism underlying the function of the F(x)$_6$LL motif in regulating GPCR trafficking, we first study how the F and LL residues in the F(x)$_6$LL motif are presented within the newly published high resolution crystal structure of β_2-AR (Cherezov et al., 2007; Rosenbaum et al., 2007). The C-terminus of β_2-AR forms an amphipathic α-helix (also known as helix 8) that projects from the seventh TM, parallel to the membrane itself. It is terminated with a cystein residue anchoring the helix to the membrane. The side chains of the F332 and LL339/340 residues project from the same face of the amphipathic α-helix back towards the membrane. However, the side chains of the F332 and LL339/340 are surrounded by quite distinct environments (Fig. 3A). The bulky, aromatic side chain of F332 appears to be buried within the

Molecular Pharmacology Fast Forward. Published on December 31, 2008 as DOI: 10.1124/mol.108.051623
This article has not been copyedited and formatted. The final version may differ from this version.

hydrophobic core of the receptor. In contrast, the branched carbon side chains of the LL339/340 residues appear to be in a more accessible region of the receptor (Fig. 3A). A surface map of the receptor indicates the solvent accessibility of the entire receptor structure in blue, and any solvent accessibility for F332 or LL339/340 in yellow. From the model it is clear that most of the LL339/340 side chains are exposed to the cytosolic space in the receptor's native environment. The side chain of F332, on the other hand, displays very little solvent accessibility (Fig. 3A). Close examination of the F332 residue reveals that its side chain is cradled by the hydrophobic residue I58 in the juxtamembrane portion of the TM1 (Fig. 3B).

We then constructed a homology model of α_{2B}-AR based on the crystal structure of β_2-AR (Cherezov et al., 2007; Rosenbaum et al., 2007). An accompanying alignment shows the high level of sequence homology in the C-termini between α_{2B}-AR and β_2-AR (Fig. 1A). The positions of the F436 and IL443/444 residues in the $F(x)_6LL$ motif of α_{2B}-AR are exactly same as those in the β_2-AR (Fig. 3C) and the F436 residue is in close proximity to the V42 residue in the TM1 (Fig. 3D). These data suggest a possible intramolecular interaction between the F332 and I58 residues in β_2-AR and between the F436 and V42 residues in α_{2B}-AR.

Effect of mutating I58 and V42 on the cell surface expression, subcellular localization and signaling of β_2-AR and α_{2B}-AR. To test the possible contribution of the I58 and V42 residues to the trafficking of β_2-AR and α_{2B}-AR, we first determined the effect of mutating I58 and V42 to alanines on the transport to the cell surface of β_2-AR and α_{2B}-AR, respectively. Wild-type receptors and their mutants were transiently expressed in HEK293T cells and their expression at the cell surface was quantified by intact cell ligand binding and

Molecular Pharmacology Fast Forward. Published on December 31, 2008 as DOI: 10.1124/mol.108.051623
This article has not been copyedited and formatted. The final version may differ from this version.

subcellular distribution as revealed by fluorescence microscopy. The cell surface expression of the I58A and V42A mutants was markedly attenuated by 90% and 61%, respectively, as compared with their wild-type counterparts (Fig. 4A).

We then determined the effect of mutation of the residue V78, which is analogous to V42 in α_{2B}-AR, on the transport of 5-HT_{2C} receptor. In contrast to α_{2B}-AR, AT1R, α_{1B}-AR and β_2-AR which have the $F(X)_6LL$ motif in the C-termini, 5-HT_{2C} receptor possesses the $Y(X)_6YL$ motif in the C-terminus. As the $5HT_{2C}$ receptor ligand [^{3}H]1-NBMeO has been well characterized in a binding assay of membrane preparations, we determined the effect of mutating the residues V78 on ligand binding of $5HT_{2C}$ receptor in the membrane preparations and compared with the α_{2B}-AR mutant V42A. Consistent with intact cell ligand binding, ligand binding of membrane preparations from cells expressing the mutant V42A was much lower than from cells expressing wild type α_{2B}-AR (Fig. 4B). In contrast, mutation of V78 to alanine significantly enhanced ligand binding of 5-HT_{2C} receptor in membrane preparations (Fig. 4B). Total receptor expression measured by flow cytometric analysis of the GFP signal showed no significant difference between wild-type and mutated receptors (data not shown). Consistent with the ligand binding data, subcellular distribution analysis revealed that the I58A mutant was completely unable to transport to the cell surface and the V42A mutant displayed a substantial intracellular retention, whereas the V78A mutant robustly expressed at the cell surface (Fig. 4C).

We then determined if mutation of V42 could influence receptor signaling by measuring ERK1/2 activation. Consistent with a significant reduction in the cell surface receptor expression as measured by ligand binding and subcellular localization, ERK1/2 activation by UK14304 in

Molecular Pharmacology Fast Forward. Published on December 31, 2008 as DOI: 10.1124/mol.108.051623
This article has not been copyedited and formatted. The final version may differ from this version.

cells expressing the V42A mutant was clearly attenuated as compared with cells expressing wild-type α_{2B}-AR (Fig. 4D).These data further indicate that the V42 residue is important for the cell surface transport of α_{2B}-AR. These data also suggest that the hydrophobic residues (such as V42) in the TM1 are essential for receptor export to the cell surface which may serve as a contact point for the F residue in the C-terminal $F(X)_6LL$ motif to coordinate tertiary structure of the receptor.

To further define the role of the possible interaction between V42 and F436 in α_{2B}-AR maturation, we examined the effect of simultaneously mutating V42 to F and F436 to V on the cell surface expression of α_{2B}-AR. Individual mutation of V42 to F or F436 to V markedly attenuated α_{2B}-AR cell surface expression (Fig. 4E). Interestingly, the cell surface expression of double mutant V42F/F436V was significantly higher than individual mutants V42F and F436V (Fig. 4E). These data suggest that swamping V42 in the TM1 and F436 in the C-termini may partially rescue α_{2B}-AR transport.

The residues V and I are conserved in the TM1s of GPCRs carrying the $F(X)_6LL$ motif in the C-termini. Since we have demonstrated that the $F(X)_6LL$ is highly conserved in the family A GPCRs and that the F residue in the motif likely interacts with the hydrophobic residue I58 in β_2-AR and V42 in α_{2B}-AR, we then searched the GPCR database to see if the I and V residues are conserved amongst the GPCRs carrying the $F(X)_6LL$ motif in the C-termini. As shown in Fig. 5, out of total 43 human GPCRs having the $F(X)_6LL$ motif in the C-termini, 39 receptors (91%) have the residues I/L/V in the TM1 in the position of I58 in β_2-AR and V42 in α_{2B}-AR (Fig. 5A and 5B). Among these GPCRs, 21 receptors (49%) have either I (16 receptors) or L residues (5 receptors) (Fig. 5A) and 18 GPCRs (42%) have V residue (Fig. 5B). Only 4

Molecular Pharmacology Fast Forward. Published on December 31, 2008 as DOI: 10.1124/mol.108.051623
This article has not been copyedited and formatted. The final version may differ from this version.

GPCRs (9%) with the $F(X)_6LL$ motif have F (3 receptors) and H residues (1 receptor) (Fig. 5C). These data strongly indicate that the hydrophobic residues I/L and V are also highly conserved among GPCR carrying the $F(X)_6LL$ motif. These data further support the important role of the potential interaction between the V/I/L residues in the TM1 and the F residue in the C-termini in modulating GPCR trafficking.

Differential interaction of the α_{2B}-AR mutants F436A and IL443/444AA with ER chaperone proteins. To further determine if the F436 and IL443/444 residues in the $F(X)_6LL$ are differentially involved in GPCR folding, we compared the interaction of α_{2B}-AR and its mutants F436A and IL443/444AA with the ER chaperones calnexin and calreticulin. Within the ER, molecular chaperones bind to nascent proteins and facilitate their proper folding. Properly folded receptors are released for export while misfolded proteins remain bound to the chaperone and are eventually targeted for degradation. Therefore, terminally misfolded receptors will display extended and robust interactions with the chaperones (Apaja et al., 2006; Lu et al., 2003; Robert et al., 2005; Ulloa-Aguirre et al., 2004). The GFP-tagged α_{2B}-AR and its mutants were transiently expressed in HEK293T cells and the receptors were then immunoprecipitated with anti-GFP antibodies. The ER chaperones calnexin and calreticulin in the GFP-immunoprecipitates were analyzed by immunoblotting. To exclude the possibility that receptor interaction with ER chaperones induced by misfolding of the receptors was caused by higher level of the receptors, wild-type and mutated α_{2B}-AR were transiently expressed in HEK293 cells using 10 times less of the plasmid DNA. A significant amount of both calnexin and calreticulin were immunoprecipitated by GFP antibodies from cells expressing α_{2B}-AR (Fig. 6), consistent with the interaction of many GPCRs with ER chaperones (Apaja et al., 2006; Lu et al.,

Molecular Pharmacology Fast Forward. Published on December 31, 2008 as DOI: 10.1124/mol.108.051623
This article has not been copyedited and formatted. The final version may differ from this version.

2003; Robert et al., 2005) confirming that chaperone interaction is a normal process in GPCR biogenesis. Interestingly, the amount of chaperones detected in the GFP immunoprecipitates from cells expressing the mutant F436A was significantly higher than from cells expressing α_{2B}-AR, but remained the same from cells expressing the IL443/444AA mutant (Fig. 6A). The amount of the α_{2B}-AR plasmid DNA used in transient transfection did not clearly alter the receptor interaction with the ER chaperones (Fig. 6). These data indicate that the F436A mutant displays a stronger, extended interaction with calnexin and calreticulin and suggest that residue F436, but not residues IL443/444, may be involved in α_{2B}-AR folding.

Rescue of the F436A and IL443/444AA mutants by low-temperature culture and DMSO treatments. To further test the hypothesis that residue F436 is involved in α_{2B}-AR folding, we investigated if the F436A and IL443/44AA mutants could be differentially rescued by low-temperature culture and DMSO treatment. HEK293T cells transfected with either α_{2B}-AR or its mutants were allowed to express for 24 h before being cultured at 30°C or treated with 2% DMSO for an additional 24 h. Cell-surface expression of the receptors was then measured by intact cell ligand binding. Both treatment conditions have been shown to rescue the expression of certain mutant GPCRs (Bailey et al., 2004; Robben et al., 2006; Tan et al., 2004), presumably by increasing the conformational stability of the receptors, thereby facilitating their passage through the ER quality control system. Low-temperature culture (Fig. 7A) and DMSO treatment (Fig. 7B) were able to significantly increase expression over control conditions of the F436A and IL443/444AA mutants. Interestingly, the F436A mutant consistently showed a greater propensity to be rescued by both low-temperature culture (Fig. 7A) and DMSO treatment (Fig. 7B) than the IL443/444AA mutant. These results indicate that the F436A and IL443/444AA mutants have

Molecular Pharmacology Fast Forward. Published on December 31, 2008 as DOI: 10.1124/mol.108.051623
This article has not been copyedited and formatted. The final version may differ from this version.

different phenotypes within the ER and suggest that the F436 and IL443/444 residues may contribute to different degrees to the assumption of an ER export competent conformation for α_{2B}-AR.

Molecular Pharmacology Fast Forward. Published on December 31, 2008 as DOI: 10.1124/mol.108.051623
This article has not been copyedited and formatted. The final version may differ from this version.

Discussion

We have previously reported that the F436 and IL443/444 residues within the C-terminus of α_{2B}-AR are required for its export from the ER (Duvernay et al., 2004; Zhou et al., 2006). Here we demonstrated that [1] the $F(x)_6LL$ motif similarly modulates ER export of α_{2B}-AR, AT1R, α_{1B}-AR and β_2-AR; [2] the function of the $F(x)_6LL$ motif in directing receptor export is dictated by their unique physiochemical properties; [3] F and LL are localized in distinct environments within the receptor superstructure and F is in close proximity to I58 in β_2-AR and V42 in α_{2B}-AR in the TM1; [4] mutation of I58 and V42 markedly reduced receptor cell surface expression; [5] I and V are highly conserved in the TM1 amongst GPCRs carrying the $F(x)_6LL$ motif; [6] α_{2B}-AR mutants F436A and IL443/444AA differentially associated with calnexin and calreticulin; [7] low temperature and chemical chaperone treatments rescued the export of F436A and IL443/444AA to different degrees. These data strongly suggest that F in the $F(x)_6LL$ motif is likely involved in receptor folding which is mediated through hydrophobic interaction with other residues in the TM1.

We first used an intact cell ligand binding assay to determine the role of the $F(x)_6LL$ motif in the cell surface expression of four GPCRs. Our data have demonstrated that mutation of the $F(x)_6LL$ motif remarkably blocked cell surface expression of α_{2B}-AR, β_2-AR, α_{1B}-AR and AT1R, resulting in extensive ER arrest. These data strongly suggest that the $F(x)_6LL$ motif plays a general role in modulating GPCR ER export.

It is apparent that the function of F436 in α_{2B}-AR export requires its unique physiochemical characteristics including hydrophobicity, polarity and the size of side chain.

Molecular Pharmacology Fast Forward. Published on December 31, 2008 as DOI: 10.1124/mol.108.051623
This article has not been copyedited and formatted. The final version may differ from this version.

First, F, Y and W are aromatic residues with different sizes. Among them, F has the smallest size and W has the largest size, whereas Y has a slightly larger size then F. The fact that the cell-surface transport of the mutant F436Y was much higher than the mutant F436W suggests that the size of F436 is likely to be the main determinant for its function. Second, the function of F436 could not be fully substituted by V, L, Y and W. As F has the highest hydrophobicity, it is possible that the hydrophobicity of F436 may also play an important role in its function. Third, F is a non-polar residue and Y and W are polar residues. It is possible that the non-polar charter of F436 is essential to its function. However, mutation of F436 to the non-polar residues V and L markedly disrupted α_{2B}-AR transport. Similarly, mutation of LL to VV and FF markedly blocked α_{2B}-AR transport, suggesting that the function of LL is dictated by its exceptional properties.

To gain insight into the molecular mechanism underlying the function of the $F(X)_6LL$ motif, we studied how F and LL are presented within the superstructure of β_2-AR and α_{2B}-AR using the newly published crystal structure of β_2-AR (Cherezov et al., 2007; Rosenbaum et al., 2007). F332 and LL339/340 in β_2-AR are surrounded by distinct environments and F332 is juxtaposed with the cytosolic end of the TM1, TM2 and TM7, in a position to possibly interact with these domains. Specifically, F332 appears to interact with I58 in the TM1. The homology model of α_{2B}-AR based on the β_2-AR structure suggests that F436 is in close proximity to V42. Indeed, mutation of I58 in β_2-AR abolished and mutation of V42 in α_{2B}-AR markedly attenuated receptor cell surface expression. More interestingly, the cell surface transport of the double mutant V42F/F436V was significantly higher than individual mutants V42F and F436V. In contrast, mutation of V78 in 5-HT_{2C} receptor, which does not have the $F(X)_6LL$ motif, markedly enhanced the ligand biding of 5-HT_{2C} receptor in membrane preparations. The molecular

Molecular Pharmacology Fast Forward. Published on December 31, 2008 as DOI: 10.1124/mol.108.051623
This article has not been copyedited and formatted. The final version may differ from this version.

mechanism underlying this phenomenon is unknown. It is possible that mutation of V78 facilities the transport of 5-HT_{2C} receptor resulting in more functional receptors or enhances 5-HT_{2C} receptor's ability to bind ligand.

The inhibitory effect of V42 mutation on α_{2B}-AR transport was not as dramatic as F436 mutation, suggesting that F436 plays a more important role than V42 in α_{2B}-AR export. It is possible that F436 may coordinate with multiple domains in addition to the TM1. In support of this concept Fritze et al. demonstrated that the highly conserved F in the helix 8 of rhodopsin interacts with Y in the NPxxY motif, responsible for maintaining the ground state conformation of the receptor and proper realignment of the helix 8 after photoisomerization (Fritze et al., 2003). In addition to V42, other hydrophobic residues such as LL in the C-terminus may also interact with F436. Nevertheless, these data suggest that F in the $F(X)_6LL$ motif coordinates a structural event required for the assumption of an ER export competent conformation.

Several studies suggest that the membrane-proximal C-terminal hydrophobic residues likely modulate GPCR folding in the ER (Robert et al., 2005; Schulein et al., 1998). To further define if F436 and IL443/444 are differentially involved in proper receptor folding, we first compared their interactions with calnexin and calreticulin, ER chaperone proteins which display stronger and extended interactions with misfolded GPCRs (Apaja et al., 2006; Lu et al., 2003; Robert et al., 2005; Ulloa-Aguirre et al., 2004). Our data indicate that F436A displayed higher levels of interaction with calnexin and calreticulin than IL443/444AA and wild-type α_{2B}-AR. We then compared the ability of F436A and IL443/444AA to be rescued by physical and chemical treatments. Successful rescue of misfolded GPCRs can be achieved by many approaches such as

Molecular Pharmacology Fast Forward. Published on December 31, 2008 as DOI: 10.1124/mol.108.051623
This article has not been copyedited and formatted. The final version may differ from this version.

chemical chaperones, pharmacological chaperones and lowering temperature (Apaja et al., 2006; Lu et al., 2003; Robert et al., 2005; Ulloa-Aguirre et al., 2004). Consistent with stronger interactions of F436A with the ER chaperones, F436A had a greater propensity to be rescued by low temperature culture and DMSO than IL443/444AA. As the defect in ER export incurred upon mutation of F436 is more easily corrected with methods that presumably tighten protein conformation, we conclude that F436 contributes to the maintenance of proper receptor conformation to a much greater degree than IL443/444.

The function of F in the $F(X)_6LL$ in modulating GPCR ER export is likely mediated through interacting with other hydrophobic residues in the TM1 (e.g. I58 in β_2-AR and V42 in α_{2B}-AR). Such intramolecular hydrophobic interactions have been demonstrated in many GPCRs to coordinate and maintain tertiary structure of the receptors (Fritze et al., 2003). Most interestingly, the hydrophobic residues V/I/L are markedly conserved amongst GPCR carrying the $F(X)_6LL$ motif, implying an important role played by these highly conserved hydrophobic residues in regulating GPCR function.

The F and LL residues in the $F(X)_6LL$ motif may dictate distinct steps involved in receptor export from the ER. Whereas our current studies suggest that F likely plays an important role in proper receptor folding, the precise mechanism underlying the function of LL remains unknown. As LL is accessible to the cytosolic space, it may function as an ER export motif which mediates receptor interaction with components of the COPII vesicles directing receptor ER export. Consistent with this possibility, the dihydrophobic residues FF mediates the ER transport of ERGIC53 and can be functionally substituted by LL. Furthermore, LL also functions

Molecular Pharmacology Fast Forward. Published on December 31, 2008 as DOI: 10.1124/mol.108.051623
This article has not been copyedited and formatted. The final version may differ from this version.

as a sorting signal at the trans-Golgi network and at the plasma membrane (Heilker et al., 1996; Hunziker et al., 1994). It is also possible that LL mediates receptor interaction with some proteins crucial for receptor ER export. Consistent with this possibility, a number of accessory proteins directly interact with the GPCR C-termini to modulate receptor export (Ferreira et al., 1996; McLatchie et al., 1998).

The identification of structural determinants for GPCR export from the ER has greatly advanced our understanding of GPCR targeting to the cell surface, yet the precise mechanisms remain to be elucidated. Recent studies have also demonstrated that the transport of GPCRs beyond their export from the ER is tightly controlled at multiple transport steps along the secretory pathway (Dong et al., 2007). The regulators involved in GPCR export have just begun to be revealed. For example, we have demonstrated that the ER-to-cell surface transport of AT1R, β-AR and α_1-AR is dependent on Rab1, Rab2 and Rab6, whereas the transport of α_{2B}-AR is dependent on Rab2, but independent of Rab1 and Rab6 (Dong and Wu, 2007; Filipeanu et al., 2004; Wu et al., 2003). We have also showed that export from the ER of different GPCRs may be differentially regulated by Sar1 (Dong et al., 2008). These data indicate that the cell surface targeting of different GPCRs may be mediated through distinct pathways. As the efficient trafficking of GPCRs and the precise positioning of specific receptors at the cell membrane are critical aspects of integrated responses of the cell to hormones and importantly, defective GPCR transport is clearly associated with the pathogenesis of a variety of human diseases (Conn et al., 2007; Morello et al., 2001). Further elucidation of the molecular mechanisms underlying the export traffic of GPCRs may provide a foundation for development of therapeutic strategies by designing specific drugs to control GPCR biosynthesis and eventually receptor function.

Molecular Pharmacology Fast Forward. Published on December 31, 2008 as DOI: 10.1124/mol.108.051623
This article has not been copyedited and formatted. The final version may differ from this version.

Acknowledgments

We are grateful to Drs. Stephen M. Lanier, John D. Hildebrandt (Medical University of South Carolina)**,** Kenneth P. Minneman, Kenneth E. Bernstein (Emory University) and David E. Nichols (Purdue University) for sharing reagents.

Molecular Pharmacology Fast Forward. Published on December 31, 2008 as DOI: 10.1124/mol.108.051623
This article has not been copyedited and formatted. The final version may differ from this version.

References

Apaja PM, Tuusa JT, Pietila EM, Rajaniemi HJ, and Petaja-Repo UE (2006) Luteinizing hormone receptor ectodomain splice variant misroutes the full-length receptor into a subcompartment of the endoplasmic reticulum. *Mol Biol Cell* **17:**2243-2255.

Arnold K, Bordoli L, Kopp J, and Schwede T (2006) The SWISS-MODEL workspace: a web-based environment for protein structure homology modelling. *Bioinformatics* **22:**195-201.

Bailey SR, Eid AH, Mitra S, Flavahan S, and Flavahan NA (2004) Rho kinase mediates cold-induced constriction of cutaneous arteries: role of alpha2C-adrenoceptor translocation. *Circ Res* **94:**1367-1374.

Bermak JC, Li M, Bullock C, and Zhou QY (2001) Regulation of transport of the dopamine D1 receptor by a new membrane-associated ER protein. *Nat Cell Biol* **3:**492-498.

Braden MR, Parrish JC, Naylor JC, and Nichols DE (2006) Molecular interaction of serotonin 5-HT2A receptor residues Phe339(6.51) and Phe340(6.52) with superpotent N-benzyl phenethylamine agonists. *Mol Pharmacol* **70**:1956-1964.

Cherezov V, Rosenbaum DM, Hanson MA, Rasmussen SG, Thian FS, Kobilka TS, Choi HJ, Kuhn P, Weis WI, Kobilka BK, and Stevens RC (2007) High-resolution crystal structure of an engineered human beta2-adrenergic G protein-coupled receptor. *Science* **318:**1258-1265.

Conn PM, Ulloa-Aguirre A, Ito J, and Janovick JA (2007) G protein-coupled receptor trafficking in health and disease: lessons learned to prepare for therapeutic mutant rescue in vivo. *Pharmacol Rev* **59:**225-250.

Dong C, Filipeanu CM, Duvernay MT, and Wu G (2007) Regulation of G protein-coupled receptor export trafficking. *Biochim Biophys Acta* **1768:**853-870.

Dong C and Wu G (2006) Regulation of anterograde transport of alpha2-adrenergic receptors by the N termini at multiple intracellular compartments. *J Biol Chem* **281:**38543-38554.

Dong C and Wu G (2007) Regulation of anterograde transport of adrenergic and angiotensin II receptors by Rab2 and Rab6 GTPases. *Cell Signal* 19:2388-2399.

Dong C, Zhou F, Fugetta EK, Filipeanu CM, and Wu G (2008) Endoplasmic reticulum export of adrenergic and angiotensin II receptors is differentially regulated by Sar1 GTPase. *Cell Signal* **20:**1035-1043.

Duvernay MT, Zhou F, and Wu G (2004) A conserved motif for the transport of G protein-coupled receptors from the endoplasmic reticulum to the cell surface. *J Biol Chem* 279:30741-30750.

Ferreira PA, Nakayama TA, Pak WL, and Travis GH (1996) Cyclophilin-related protein RanBP2 acts as chaperone for red/green opsin. *Nature* **383:**637-640.

Filipeanu CM, Zhou F, Claycomb WC, and Wu G (2004) Regulation of the cell surface expression and function of angiotensin II type 1 receptor by Rab1-mediated endoplasmic reticulum-to-Golgi transport in cardiac myocytes. *J Biol Chem* **279:**41077-41084.

Filipeanu CM, Zhou F, Fugetta EK, and Wu G (2006) Differential regulation of the cell-surface targeting and function of beta- and alpha1-adrenergic receptors by Rab1 GTPase in cardiac myocytes. *Mol Pharmacol* **69:**1571-1578.

Fritze O, Filipek S, Kuksa V, Palczewski K, Hofmann KP, and Ernst OP (2003) Role of the conserved NPxxY(x)5,6F motif in the rhodopsin ground state and during activation. *Proc Natl Acad Sci U S A* **100:**2290-2295.

Heilker R, Manning-Krieg U, Zuber JF, and Spiess M (1996) In vitro binding of clathrin adaptors to sorting signals correlates with endocytosis and basolateral sorting. *EMBO J* **15:**2893-2899.

Heymann JA and Subramaniam S (1997) Expression, stability, and membrane integration of truncation mutants of bovine rhodopsin. *Proc Natl Acad Sci U S A* **94:**4966-4971.

Hunziker W and Fumey C (1994) A di-leucine motif mediates endocytosis and basolateral sorting of macrophage IgG Fc receptors in MDCK cells. *EMBO J* **13:**2963-2969.

Lu M, Echeverri F, and Moyer BD (2003) Endoplasmic reticulum retention, degradation, and aggregation of olfactory G-protein coupled receptors. *Traffic* **4:**416-433.

Ma D, Zerangue N, Lin YF, Collins A, Yu M, Jan YN, and Jan LY (2001) Role of ER export signals in controlling surface potassium channel numbers. *Science* **291:**316-319.

McLatchie LM, Fraser NJ, Main MJ, Wise A, Brown J, Thompson N, Solari R, Lee MG, and Foord SM (1998) RAMPs regulate the transport and ligand specificity of the calcitonin-receptor-like receptor. *Nature* **393:**333-339.

Mizrachi D and Segaloff DL (2004) Intracellularly located misfolded glycoprotein hormone receptors associate with different chaperone proteins than their cognate wild-type receptors. *Mol Endocrinol* **18:**1768-1777.

Morello JP and Bichet DG (2001) Nephrogenic diabetes insipidus. *Annu Rev Physiol* **63:**607-630.

Morello JP, Salahpour A, Petaja-Repo UE, Laperriere A, Lonergan M, Arthus MF, Nabi IR, Bichet DG, and Bouvier M (2001) Association of calnexin with wild type and mutant AVPR2 that causes nephrogenic diabetes insipidus. *Biochemistry* **40:**6766-6775.

Nishimura N, and Balch WE (1997) A di-acidic signal required for selective export from the endoplasmic reticulum. *Science* **277:**556-558.

Pankevych H, Korkhov V, Freissmuth M, and Nanoff C (2003) Truncation of the A1 adenosine receptor reveals distinct roles of the membrane-proximal carboxyl terminus in receptor folding and G protein coupling. *J Biol Chem* **278:**30283-30293.

Petaja-Repo UE, Hogue M, Laperriere A, Walker P, and Bouvier M (2000) Export from the endoplasmic reticulum represents the limiting step in the maturation and cell surface expression of the human delta opioid receptor. *J Biol Chem* **275:**13727-13736.

Pierce KL, Premont RT, and Lefkowitz RJ (2002) Seven-transmembrane receptors. *Nat Rev Mol Cell Biol* **3:**639-650.

Robben JH, Sze M, Knoers NV, and Deen PM (2006) Rescue of vasopressin V2 receptor mutants by chemical chaperones: specificity and mechanism. *Mol Biol Cell* **17:**379-386.

Robert J, Auzan C, Ventura MA, and Clauser E (2005) Mechanisms of cell-surface rerouting of an endoplasmic reticulum-retained mutant of the vasopressin V1b/V3 receptor by a pharmacological chaperone. *J Biol Chem* **280:**42198-42206.

Rosenbaum DM, Cherezov V, Hanson MA, Rasmussen SG, Thian FS, Kobilka TS, Choi HJ, Yao XJ, Weis WI, Stevens RC, and Kobilka BK (2007) GPCR engineering yields high-resolution structural insights into beta2-adrenergic receptor function. *Science* **318:**1266-1273.

Schulein R, Hermosilla R, Oksche A, Dehe M, Wiesner B, Krause G, and Rosenthal W (1998) A dileucine sequence and an upstream glutamate residue in the intracellular carboxyl terminus of the vasopressin V2 receptor are essential for cell surface transport in COS.M6 cells. *Mol Pharmacol* **54:**525-535.

Tan CM, Brady AE, Nickols HH, Wang Q, and Limbird LE (2004) Membrane trafficking of G protein-coupled receptors. *Annu Rev Pharmacol Toxicol* **44:**559-609.

Tetsuka M, Saito Y, Imai K, Doi H, and Maruyama K (2004) The basic residues in the membrane-proximal C-terminal tail of the rat melanin-concentrating hormone receptor 1 are required for receptor function. *Endocrinology* **145:**3712-3723.

Ulloa-Aguirre A, Janovick JA, Brothers SP, and Conn PM (2004) Pharmacologic rescue of conformationally-defective proteins: implications for the treatment of human disease. *Traffic* **5:**821-837.

von Zastrow M (2003) Mechanisms regulating membrane trafficking of G protein-coupled receptors in the endocytic pathway. *Life Sci* **74:**217-224.

Wang X, Matteson J, An Y, Moyer B, Yoo JS, Bannykh S, Wilson IA, Riordan JR, and Balch WE (2004) COPII-dependent export of cystic fibrosis transmembrane conductance regulator from the ER uses a di-acidic exit code. *J Cell Biol* **167:**65-74.

Wu G, Zhao G, and He Y (2003) Distinct pathways for the trafficking of angiotensin II and adrenergic receptors from the endoplasmic reticulum to the cell surface: Rab1-independent transport of a G protein-coupled receptor. *J Biol Chem* **278:**47062-47069.

Zhou F, Filipeanu CM, Duvernay MT, and Wu G (2006) Cell-surface targeting of alpha2-adrenergic receptors - inhibition by a transport deficient mutant through dimerization. *Cell Signal* **18:**318-327.

Molecular Pharmacology Fast Forward. Published on December 31, 2008 as DOI: 10.1124/mol.108.051623
This article has not been copyedited and formatted. The final version may differ from this version.

Footnotes

This work was supported by National Institutes of Health grants R01GM076167 (to G. Wu) and R21MH078454 (to C.D. Nichols).

Molecular Pharmacology Fast Forward. Published on December 31, 2008 as DOI: 10.1124/mol.108.051623
This article has not been copyedited and formatted. The final version may differ from this version.

Legends for Figures

Fig. 1. Effect of the mutation of the $F(X)_6LL$ motif on the transport of α_{2B}-AR, AT1R, α_{1B}-AR and β_2-AR to the cell surface. A, a sequence alignment of the membrane-proximal C-terminal (CT) regions of α_{2B}-AR, AT1R, α_{1B}-AR and β_2-AR carrying the $F(X)_6LL$ motif. The F and LL residues spaced by six residues are bolded. TM7 – 7th transmembrane domain. B, quantification of the cell-surface and total expression of α_{2B}-AR, AT1R, α_{1B}-AR and β_2-AR and their mutants (α_{2B}-ARm, AT1Rm, α_{1B}-ARm and β_2-ARm) in which the $F(X)_6LL$ motif was mutated. HEK293T cells cultured on 6-well plates were transfected with each of the receptors and then split onto 12-well plates. The cell-surface expression of α_{2B}-AR, AT1R, α_{1B}-AR and β_2-AR was measured by intact cell binding assays using [^{3}H]-RX821002, [^{125}I]-Ang II, [7-methoxy-^{3}H]-prazosin and [^{3}H]-CGP12177, respectively, as described under "Materials and Methods". The mean values of specific ligand binding from cells transfected with α_{2B}-AR, α_{2B}-ARm, AT1R, AT1Rm, α_{1B}-AR, α_{1B}-ARm, β_2-AR and β_2-ARm were 23,327 ± 591, 2,799 ± 126, 9,734 ± 342, 876 ± 155, 31,142 ± 963, 4,048 ± 625, 38,560 ± 2,432 and 5,784 ± 289 cpm, respectively. Total receptor expression was determined by flow cytometry measuring the GFP signal as described in the "Materials and Methods". The data shown are percentages of the mean value obtained from cells transfected with wild-type receptors (WT) and are presented as the mean ± S.E. of at least three separate experiments. *, $p<0.05$ *versus* cells transfected with wild-type receptors. C, cAMP production in cells expressing β_2-AR and β_2-ARm. HEK293T cells were cultured on 6-well plates and transfected with the pEGFP-N1 vector (GFP), GFP-tagged β_2-AR or β_2-ARm. The cells were then stimulated with ISO at a concentration of 10 μM for 5 min. cAMP production was measured as described under "Materials and Methods". The data shown are expressed as percentages of the cAMP production obtained in cells transfected with β_2-AR and stimulated

with ISO and presented as the mean ± S.E. of three separate experiments. In a typical experiment, the cAMP concentration after stimulation with ISO in cells expressing wild-type β_2-AR is 2331 fmol/well. *, $p < 0.05$ versus cells transfected with β_2-AR. D, subcellular localization of β_2-AR and α_{1B}-AR and their mutants. GFP-conjugated wild-type and mutated receptors were transiently expressed in HEK293T cells, and their subcellular distribution was revealed by fluorescence microscopy as described under "Materials and Methods". E, co-localization of α_{1B}-ARm with the ER marker DsRed2-ER. HEK293T cells were co-transfected with the GFP-tagged α_{1B}-ARm together with the plasmid pDsRed2-ER and the subcellular distribution and co-localization of the receptor with DsRed2-ER were revealed by fluorescence microscopy as described under "Materials and Methods". *Green*, α_{1B}-AR tagged with GFP; *red*, the ER marker DsRed2-ER; *yellow*, co-localization of the receptor with the ER; *blue*, DNA staining by 4,6-diamidino-2-phenylindole (nuclei). The data shown in D and E are representative images of at lease three independent experiments. Scale bar, 10 μm.

Fig. 2. Effect of substitution of F436 and IL443/444 with different hydrophobic residues on α_{2B}-AR transport to the cell surface. A, specific [^{3}H]-RX821002 binding on intact HEK293T cells transfected with α_{2B}-AR and its mutants. HEK293T cells cultured on 6-well plates were transfected with GFP-conjugated α_{2B}-AR or individual mutants. The cell-surface expression of the receptors was measured by intact cell ligand binding as described under "Materials and Methods". The data are presented as the percentage of specific binding from cells transfected with α_{2B}-AR and are presented as the mean ± S.E. of three separate experiments. *, $p < 0.05$ versus cells transfected with α_{2B}-AR. B, subcellular localization of α_{2B}-AR and its mutants revealed by detecting GFP fluorescence.

Molecular Pharmacology Fast Forward. Published on December 31, 2008 as DOI: 10.1124/mol.108.051623
This article has not been copyedited and formatted. The final version may differ from this version.

Fig. 3. Structural analysis of the $F(X)_6LL$ motif in β_2-AR and α_{2B}-AR. A, representation of the "Connelly Surface" or the surface traced out by water molecules interacting with exposed portions of the protein based on the crystal structure of β_2-AR. The Connelly surface for the entire protein is represented in blue. Those portions of F332 and LL339/340 with the potential for interaction with water molecules are shown in yellow. B, a close view of the F332 and LL339/340 residues and their intra-molecular environments. The first transmembrane domain (TM1) is colored in blue, the seventh transmembrane domain (TM7) in red, and the C-terminus (CT) in yellow. Carbon, oxygen, and nitrogen in residues are labeled in green, red and blue, respectively. The distance between F332 of the C-terminus and I58 of the first transmembrane domain is labeled in angstroms. C, homology modeling of α_{2B}-AR based on the crystal structure of β_2-AR as in A. D, positions of the F436, IL4433/444 and V42 residues and their intra-molecular environments in α_{2B}-AR as in B for β_2-AR.

Fig. 4. Effect of mutation of the I58, V42 and V78 residues on the cell surface transport and subcellular localization of β_2-AR, α_{2B}-AR and 5-HT_{2C} receptor, respectively. A, quantitation of the cell-surface expression of β_2-AR and α_{2B}-AR and their mutants. HEK293T cells cultured on 6-well plates were transfected with GFP-conjugated receptors and then split onto 12-well plates. The cell-surface expression of the receptors was measured by intact cell binding assays as described under "Experimental procedures". The mean values of specific ligand binding were 37,843 ± 844, 3,238 ± 289, 23,663 ± 597 and 9,254 ± 200 cpm from cells transfected with β_2-AR, I58A, α_{2B}-AR and V42A, respectively. The data shown are the percentage of the mean value obtained from cells transfected with wild-type receptor (WT) and are presented as the mean ± S.E. of three experiments. B, Specific ligand binding to membrane fractions prepared

Molecular Pharmacology Fast Forward. Published on December 31, 2008 as DOI: 10.1124/mol.108.051623
This article has not been copyedited and formatted. The final version may differ from this version.

from the cells transfected with α_{2B}-AR and 5-HT_{2C} receptor and their mutants. HEK293T cells were transiently transfection with GFP-tagged α_{2B}-AR, 5-HT_{2C} receptor or their mutants (V42A and V78A). The membrane fractions were incubated with the radioligands [^{3}H]-RX-821002 or [^{3}H]1-NBMeO as described under "Materials and Methods". The mean values of specific ligand binding were 22,324 ± 1102, 9,376 ± 1116, 10,196 ± 660 and 19,085 ± 312 cpm (mean ± S.E., n=3-4) from cells transfected with α_{2B}-AR, V42A, 5-HT_{2C} receptor and V78A, respectively. C, subcellular distribution of β_2-AR, α_{2B}-AR and 5-HT_{2C} receptor and their mutants. HEK293T cells transfected with GFP-conjugated receptors were split onto coverslips and subcellular distribution of the receptors was revealed by detecting GFP fluorescence as described under "Materials and Methods". The data are representative images of at least four independent experiments. Scale bar, 10 μm. C, ERK1/2 activation by α_{2B}-AR and its mutant. HEK293T cells cultured on 6-well plates were transfected with α_{2B}-AR or V42A and stimulated with UK14304 at a concentration of 1 μM for 5 min. ERK1/2 activation was determined by Western blot analysis using phosphospecific ERK1/2 antibodies. *Left upper panel*, a representative blot of ERK1/2 activation; *left lower panel*, total ERK1/2 expression; *Right panel*, quantitative data expressed as the percentage of the ERK1/2 activation obtained from cells transfected with α_{2B}-AR and are presented as the mean ± S.E. of three separate experiments. E, quantitation of the cell-surface expression of α_{2B}-AR and their mutants V42F, F436V and V42F/F436V. *, $p < 0.05$ versus cells transfected with their respective wild-type receptors; **, $p < 0.05$ versus cells transfected with V42F or F436V.

Fig. 5. The conserved F/I/L in the first transmembrane domain of GPCRs. The data were constructed from www.gpcr.org. Only human sequences are shown. A, GPCRs containing the I

Molecular Pharmacology Fast Forward. Published on December 31, 2008 as DOI: 10.1124/mol.108.051623
This article has not been copyedited and formatted. The final version may differ from this version.

and L residues in the first transmembrane domains (TM1) and the $F(X)_6LL$ motif in the C-termini (CT). B, GPCRs containing the V residue in the TM1 and the $F(X)_6LL$ motif; C, GPCRs containing the $F(X)_6LL$ motif in the C-termini but without V, I or L in the TM1. β_1-AR, β_1-adrenergic receptor; β_2-AR, β_2-adrenergic receptor; β_3-AR, β_3-adrenergic receptor; α_{1B}-AR, α_{1B}-adrenergic receptor; α_{1D}-AR, α_{1D}-adrenergic receptor; α_{2A}-AR, α_{2A}-adrenergic receptor; α_{2B}-AR, α_{2B}-adrenergic receptor; α_{2C}-AR, α_{2C}-adrenergic receptor; D2DR, dopamine D(2) receptor; D3DR, dopamine D(3) receptor; D5DR, dopamine D(5) receptor; 5HT1A, human 5-hydroxytryptamine 1A receptor; 5HT1E, 5-hydroxytryptamine 1E receptor; TAAR2, trace amine-associated receptor 2; ACM1, muscarinic acetylcholine receptor M1; ACM2, muscarinic acetylcholine receptor M2; ACM3, muscarinic acetylcholine receptor M3; ACM4, muscarinic acetylcholine receptor M4; ACM5, muscarinic acetylcholine receptor M5; AT1R, angiotensin II type 1 receptor; CXCR1, C-X-C chemokine receptor type 1; CXCR2, C-X-C chemokine receptor type 2; CXCR3, C-X-C chemokine receptor type 3; CXCR5, C-X-C chemokine receptor type 5; CKRA, human C-C chemokine receptor type 10; PRLHR, prolactin-releasing hormone receptor; P2Y6, P2Y purinoceptor 6; SS1R, somatostatin receptor type 1; GPR7, neuropeptides B/W receptor type 1; GPR8, neuropeptides B/W receptor type 2; LSHR, lutropin-choriogonadotropic hormone receptor precursor; TSHR, thyrotropin receptor precursor; FSHR, follicle stimulating hormone receptor precursor. AA2A, adenosine A2a receptor; AA2B, adenosine A2b receptor; AA3R, adenosine A3 receptor; H1R, histamine H1 receptor; ML1A, melatonin type 1A receptor; ML1B, melatonin type 1B receptor.

Fig. 6. Differential interaction of the α_{2B}-AR mutants F436A and IL443/444AA with ER chaperones. A, immunoblot analysis of the ER chaperones calnexin and calreticulin and α_{2B}-AR

Molecular Pharmacology Fast Forward. Published on December 31, 2008 as DOI: 10.1124/mol.108.051623
This article has not been copyedited and formatted. The final version may differ from this version.

in the GFP immunoprecipitates. HEK293T cells were cultured on 10-cm dishes and then transfected with 3 μg (left panel) and 0.3 μg (right panel) of the plasmid DNA of GFP-conjugated α_{2B}-AR, F436A or IL443/444AA and the receptors were immunoprecipitated with anti-GFP antibodies as described under "Experimental procedures". Calnexin (upper panel), calreticulin (middle panel) and α_{2B}-AR (lower panel) in the GFP-immunoprecipitates were revealed by immunoblotting using antibodies against calnexin, calreticulin and GFP, respectively. The data shown are representative of three independent experiments. B, quantitation of immunoblots from panel A. The data shown are the percentage of the mean value obtained from cells transfected with wild-type α_{2B}-AR and are presented as the means ± S.E. of three separate experiments *, $p < 0.05$ versus cells transfected with wild-type α_{2B}-AR.

Fig. 7. Rescue of the cell-surface expression of the α_{2B}-AR mutants F436A and IL443/444AA by low-temperature culture and treatment with DMSO. A, specific [^{3}H]-RX821002 binding to intact HEK293T cells transfected with α_{2B}-AR, F436A or IL443/444AA and cultured at 37°C and 30°C for 40 h. The cell-surface expression of the receptors was measured by using [^{3}H]-RX821002 at a concentration of 20 nM in duplicate. *Left panel* - the data shown are fold increase in receptor cell-surface expression at 30°C over 37°C and are presented as the mean ± S.E. of three separate experiments. *, $p<0.05$ versus wild-type α_{2B}-AR. B, specific [^{3}H]-RX821002 binding to intact HEK293T cells transfected with α_{2B}-AR, F436A or IL443/444AA and treated with 2% DMSO for 24 h. *Left panel* - the data shown are fold increase in cell-surface receptor expression after DMSO treatment and are presented as the mean ± S.E. of three separate experiments. *, $p<0.05$ versus wild-type α_{2B}-AR.

Molecular Pharmacology Fast Forward. Published on December 31, 2008 as DOI: 10.1124/mol.108.051623
This article has not been copyedited and formatted. The final version may differ from this version.

Fig. 1

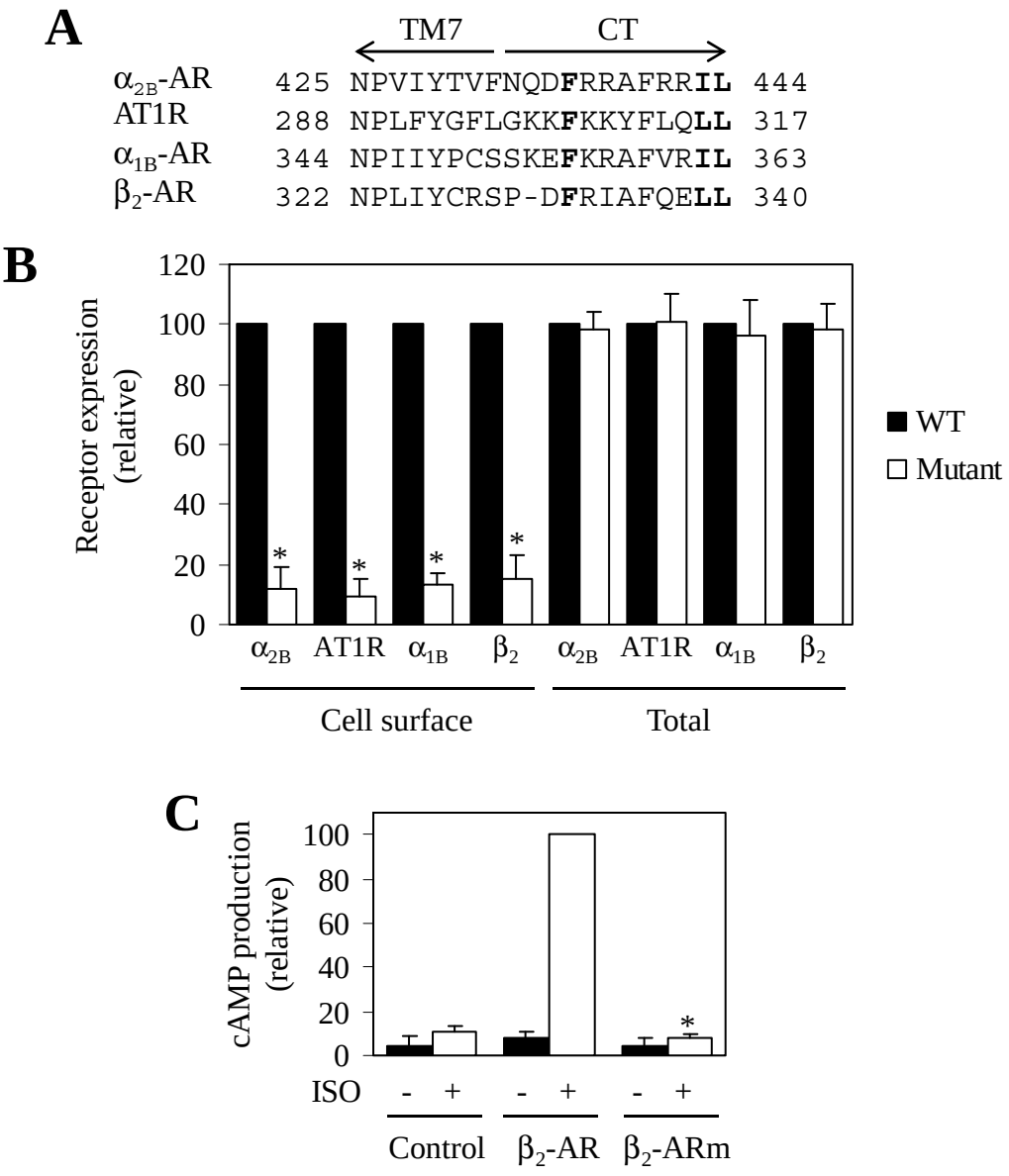

Molecular Pharmacology Fast Forward. Published on December 31, 2008 as DOI: 10.1124/mol.108.051623
This article has not been copyedited and formatted. The final version may differ from this version.

Fig. 1

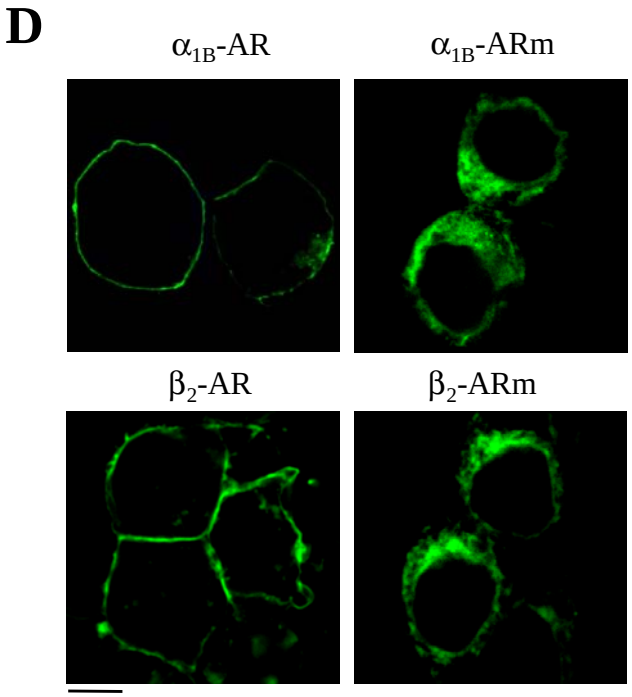

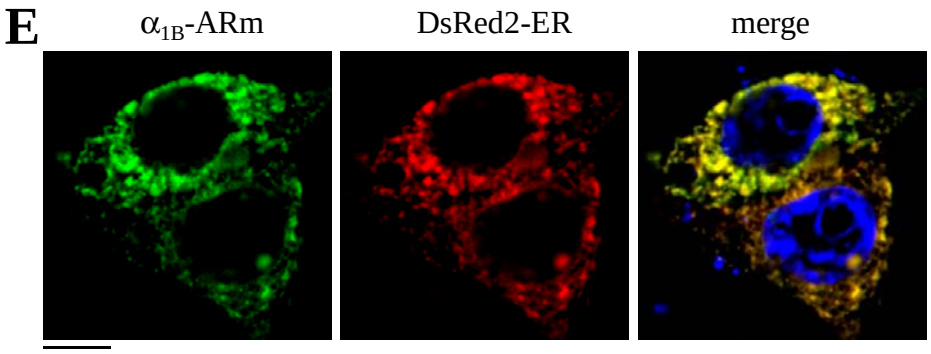

Molecular Pharmacology Fast Forward. Published on December 31, 2008 as DOI: 10.1124/mol.108.051623
This article has not been copyedited and formatted. The final version may differ from this version.

Fig. 2

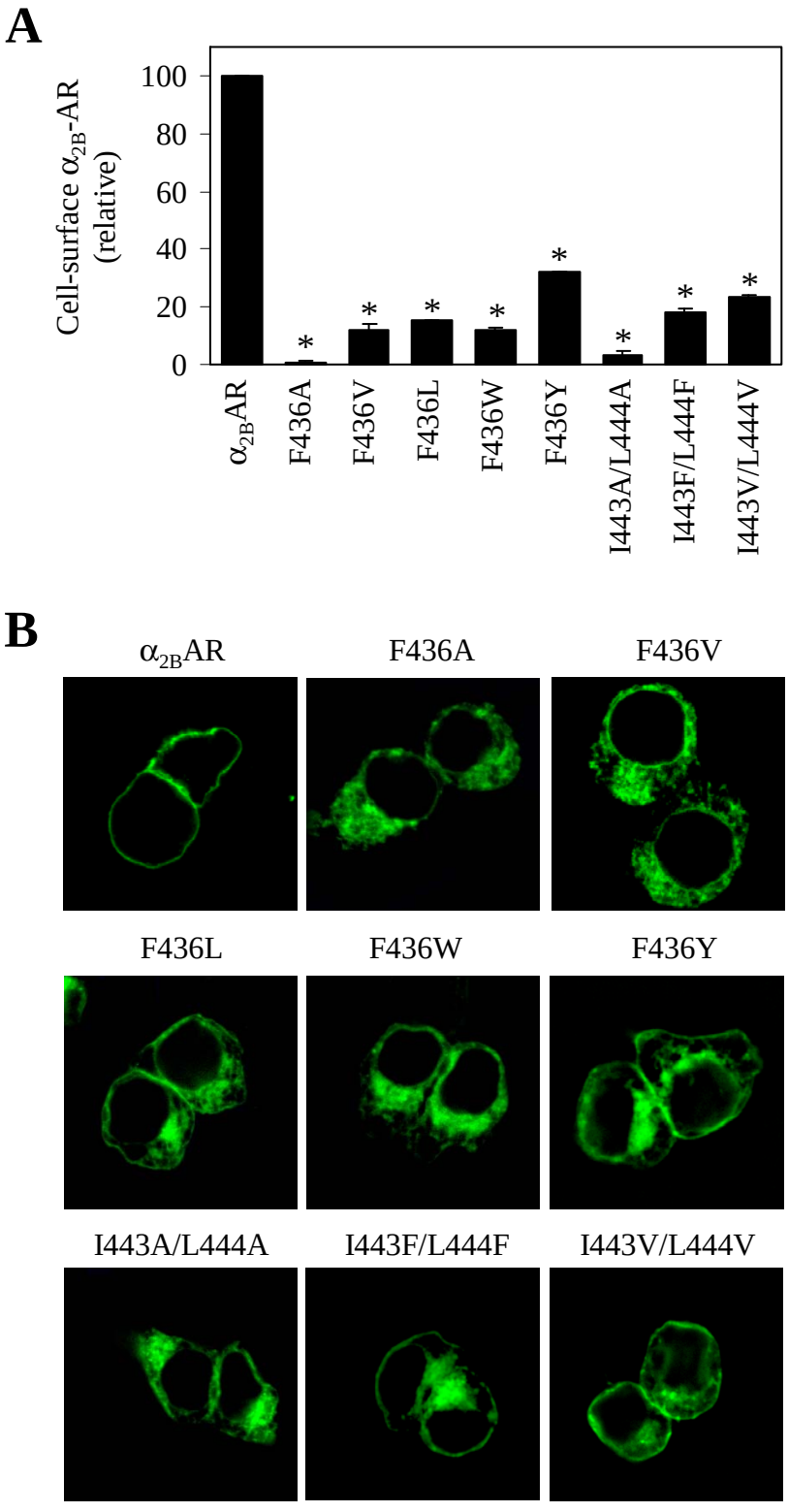

Molecular Pharmacology Fast Forward. Published on December 31, 2008 as DOI: 10.1124/mol.108.051623
This article has not been copyedited and formatted. The final version may differ from this version.

Fig. 3

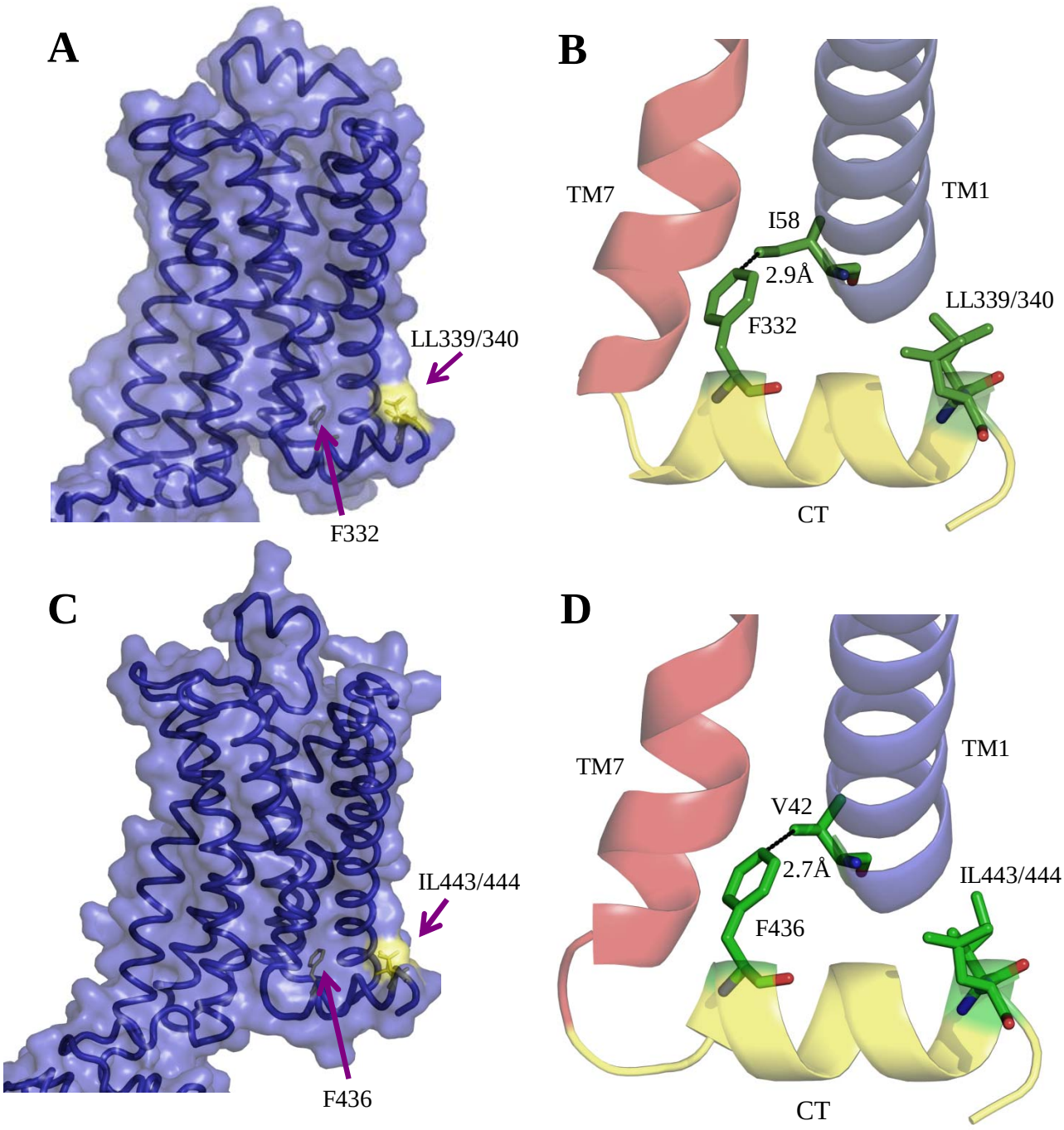

Molecular Pharmacology Fast Forward. Published on December 31, 2008 as DOI: 10.1124/mol.108.051623
This article has not been copyedited and formatted. The final version may differ from this version.

Fig. 4

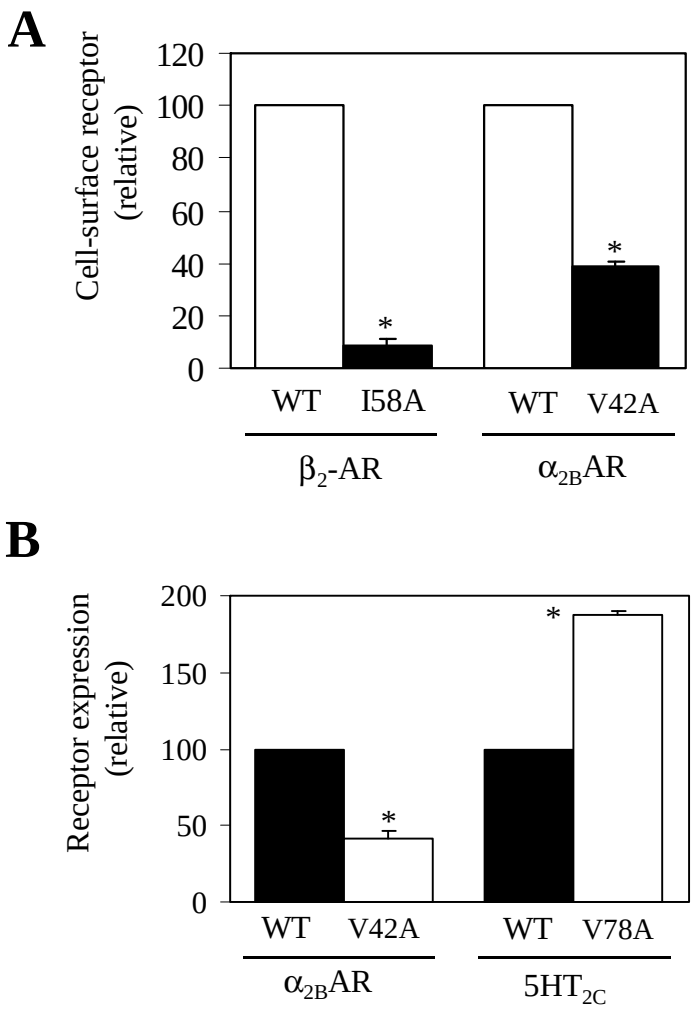

Molecular Pharmacology Fast Forward. Published on December 31, 2008 as DOI: 10.1124/mol.108.051623
This article has not been copyedited and formatted. The final version may differ from this version.

Fig. 4

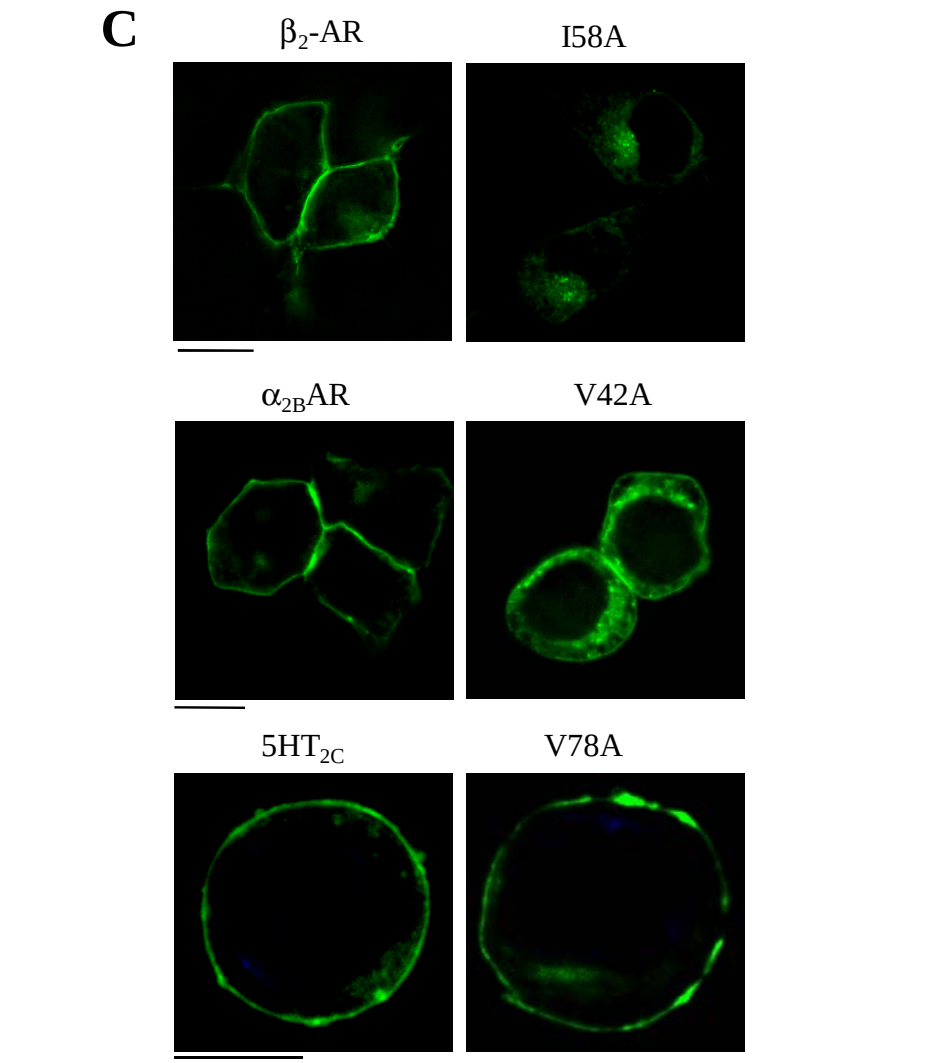

Molecular Pharmacology Fast Forward. Published on December 31, 2008 as DOI: 10.1124/mol.108.051623
This article has not been copyedited and formatted. The final version may differ from this version.

Fig. 5

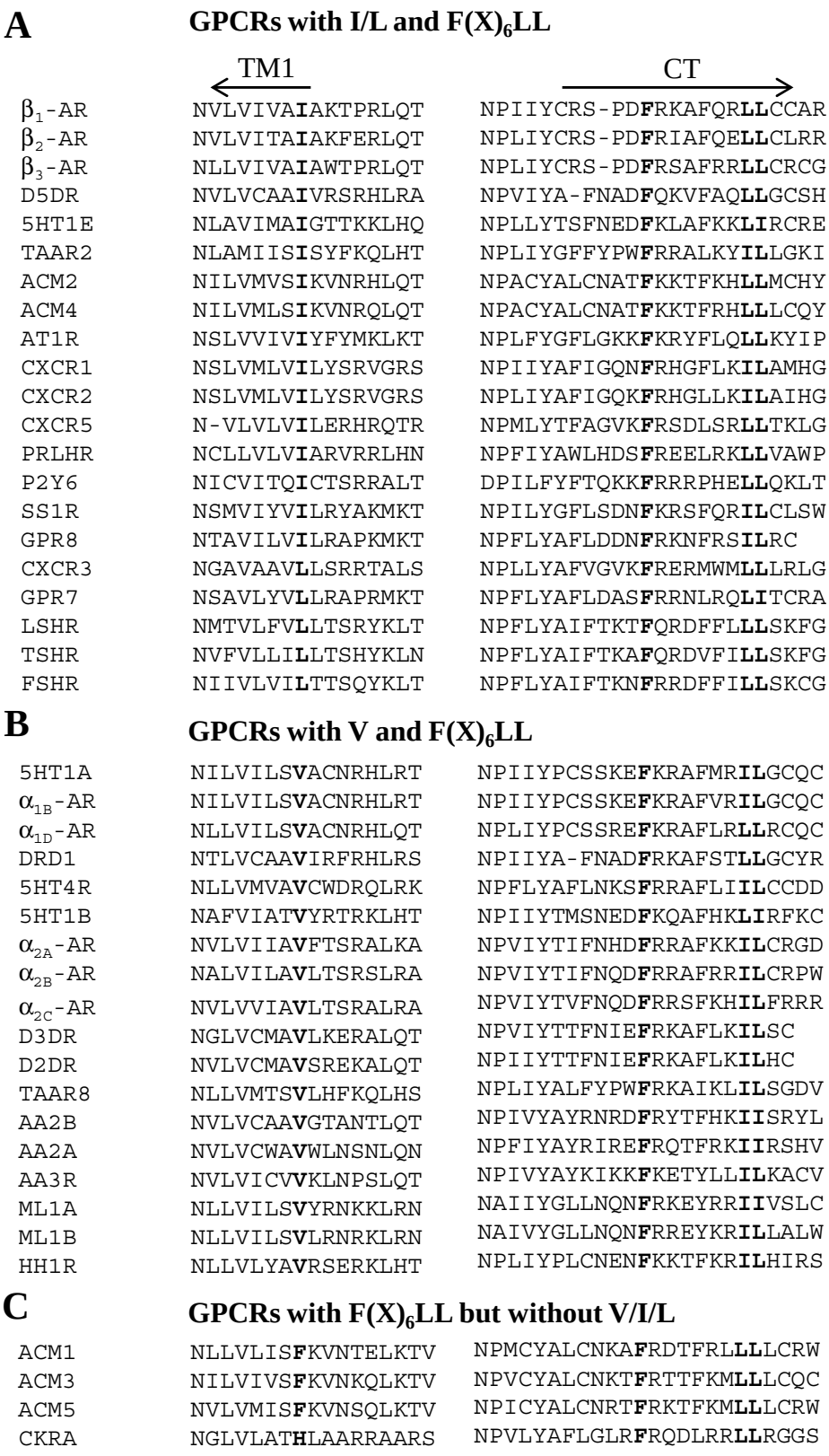

Molecular Pharmacology Fast Forward. Published on December 31, 2008 as DOI: 10.1124/mol.108.051623
This article has not been copyedited and formatted. The final version may differ from this version.

Fig. 6

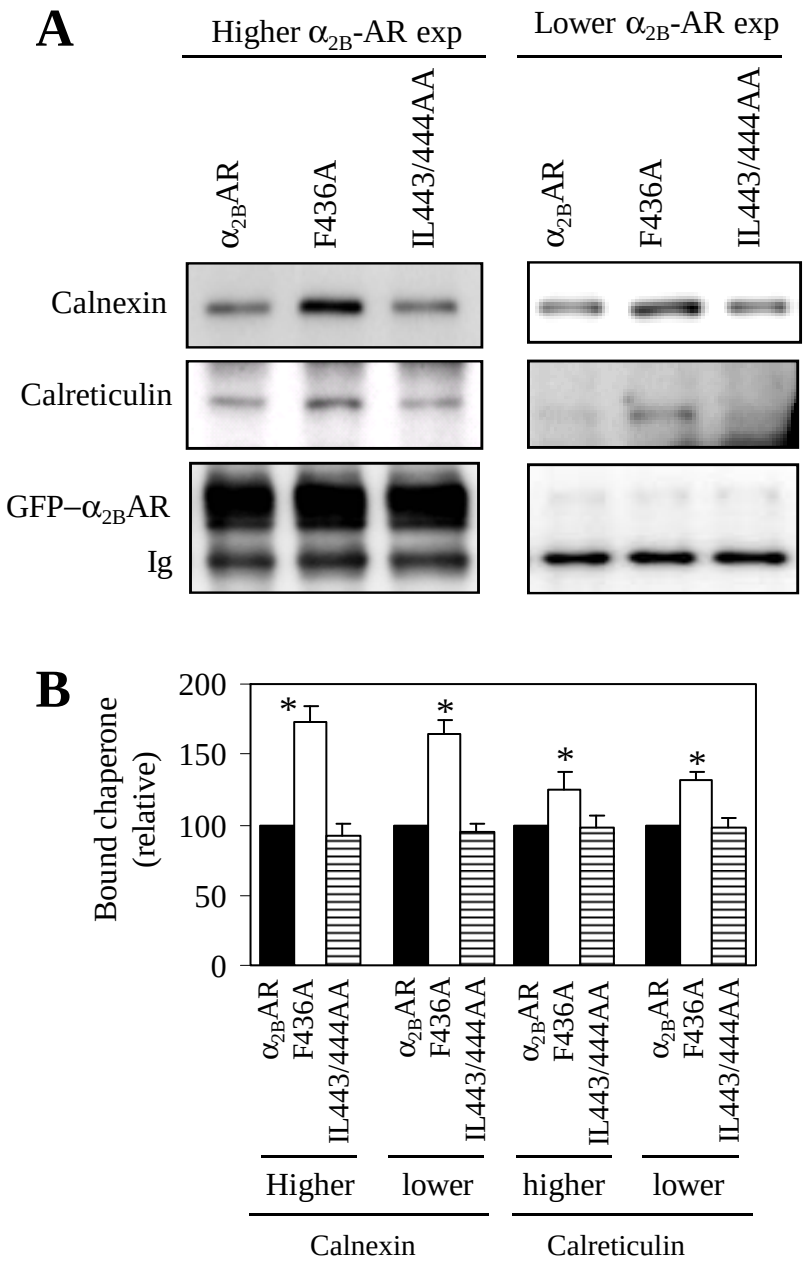

Molecular Pharmacology Fast Forward. Published on December 31, 2008 as DOI: 10.1124/mol.108.051623
This article has not been copyedited and formatted. The final version may differ from this version.

Fig. 7